AFRL-ML-TY-TR-1998-4531

HYDROTHERMOLYSIS OF ENERGETIC MATERIALS: SAFETY AND CONTINUOUS PROCESS PARAMETERS

INDIRA S. JAYAWEERA
DAVID S. ROSS
THEODORE MILL
PAUL PENWELL

SRI INTERNATIONAL
333 RAVENSWOOD AVENUE
MENLO PARK CA 94025-3493

JUNE 1998

Approved for Public Release: Distribution Unlimited.

AIR FORCE RESEARCH LABORATORY
MATERIALS & MANUFACTURING DIRECTORATE
AIRBASE & ENVIRONMENTAL TECHNOLOGY DIVISION
TYNDALL AFB FL 32403-5323

NOTICES

WHEN GOVERNMENT DRAWINGS, SPECIFICATIONS, OR OTHER DATA INCLUDED IN THIS DOCUMENT FOR ANY PURPOSE OTHER THAN GOVERNMENT PROCUREMENT DOES NOT IN ANY WAY OBLIGATE THE US GOVERNMENT. THE FACT THAT THE GOVERNMENT FORMULATED OR SUPPLIED THE DRAWINGS, SPECIFICATIONS, OR OTHER DATA DOES NOT LICENSE THE HOLDER OR ANY OTHER PERSON OR CORPORATION, OR CONVEY ANY RIGHTS OR PERMISSION TO MANUFACTURE, USE, OR SELL ANY PATENTED INVENTION THAT MAY RELATE TO THEM.

THIS REPORT IS RELEASABLE TO THE NATIONAL TECHNICAL INFORMATION SERVICE (NTIS). AT NTIS, IT WILL BE AVAILABLE TO THE GENERAL PUBLIC, INCLUDING FOREIGN NATIONS.

THIS TECHNICAL REPORT HAS BEEN REVIEWED AND IS APPROVED FOR PUBLICATION.

JAMES A. HURLEY
Program Manager

CHRISTINE WAGENER-HULME, Lt Col, USAF, BSC
Chief, Environmental Technology Development Branch

ANDREW D. POULIS
Scientific & Technical
Information Program Manager

NEIL J. LAMB, Col, USAF, BSC
Chief, Airbase & Environmental Technology Division

IF YOUR ADDRESS HAS CHANGED, IF YOU WISH TO BE REMOVED FROM OUR MAILING LIST, OR IF THE ADDRESSEE IS NO LONGER EMPLOYED BY YOUR ORGANIZATION, PLEASE NOTIFY AFRL/MLQP, TYNDALL AFB, FLORIDA 32403-5323, TO HELP MAINTAIN A CURRENT MAILING LIST.

Do not return copies of this report unless contractual obligations or notice on a specific document requires its return.

REPORT DOCUMENTATION PAGE

Form Approved
OMB No. 0704-0188

1. AGENCY USE ONLY *(Leave blank)*	2. REPORT DATE	3. REPORT TYPE AND DATES COVERED
	June 1998	Final report: 16 October 1994 - 16 June 1996

4. TITLE AND SUBTITLE

Hydrothermolysis of Energetic Materials: Safety and Continuous Process Parameters

5. FUNDING NUMBERS

F08637-94-C-6050

6. AUTHOR(S)

Indira S. Jayaweera, David S. Ross, Theodore Mill and Paul Penwell

7. PERFORMING ORGANIZATION NAME(S) AND ADDRESS(ES)

SRI International
333 Ravenswood Avenue
Menlo Park CA 94025-3493

8. PERFORMING ORGANIZATION REPORT NUMBER

SRI Project 6209

9. SPONSORING/MONITORING AGENCY NAME(S) AND ADDRESS(ES)

AFRL/MLQE (Stop 37)
139 Barnes Drive, Suite 2
Tyndall AFB FL 32403-5323

10. SPONSORING/MONITORING AGENCY REPORT NUMBER

AFRL-ML-TY-TR-1998-4531

11. SUPPLEMENTARY NOTES

Program Manager: James A. Hurley, AFRL/MLQE, (850) 283-6243; DSN 523-6243

12a. DISTRIBUTION AVAILABILITY STATEMENT

Approved for Public Release: Distribution Unlimited.

12b. DISTRIBUTION CODE

A

13. ABSTRACT *(Maximum 200 words)*

SRI conducted a study on the hydrothermolytic disposal of energetic materials (EMs) using a continuous flow reactor which was designed, assembled and tested in studies of the hydrothermolysis of amonium picrate at 360°C. The dissolution study showed that the TNT solubility in water increased by a factor of about 200 from 25°C to 200°C. The literature shows that the solubility of benzene in water increases by a factor of about 50 over the same interval and benzene becomes completely soluble at about 300°C. Therefore, the complete dissolution of TNT in water at temperatures no greater than 300°C. Calculations of the critical radii for explosion were made for TNT, HMS, and PETN at 200-350°C based on relations for kinetics of self heating. TNT has a critical radius of 0.019cm at 350°C, meaning that spherical particles exceeding this radius will self heat to explosion at 350°C.

14. SUBJECT TERMS	15. NUMBER OF PAGES
	42
	16. PRICE CODE

17. SECURITY CLASSIFICATION OF REPORT	18. SECURITY CLASSIFICATION OF THIS PAGE	19. SECURITY CLASSIFICATION OF ABSTRACT	20. LIMITATION OF ABSTRACT
Unclassified	Unclassified	Unclassified	UL

CLASSIFIED BY:

DECLASSIFY ON:

ABSTRACT

SRI has conducted a study on the hydrothermolytic disposal of energetic materials (EMs), focusing on a demonstration of the safety and environmental acceptability of the concept. The technology evolved from the recognition that 1) the explosive hazard arises from self heating in the bulk, undiluted EM, 2) under hydrothermal conditions water can be a good solvent for organic materials and EMs in particular, and 3) under those conditions EMs are converted to products that are either directly exhaustible or easily treated by conventional secondary techniques. Thus the disposal hazard should vanish if the bulk explosive is dissolved in water, while thermal destruction takes place concurrently.

The work described in this report includes determination of TNT solubility in water at elevated temperatures, a calorimetric study of the destruction of TNT both as a dry solid and suspended in water, the design and assembly of a bench-scale continuous reactor to operate under hydrothermal conditions, and a study of the hydrothermolysis of ammonium picrate in the reactor.

In the dissolution study we found that the solubility of TNT in water increased by a factor of about 200 from 25°C to 200°C to a value of about 1.5 wt%. Accounts in the literature show that the solubility of benzene in water increases by a factor of about 50 over the same interval and benzene becomes completely soluble at about 300°C. We therefore expect complete dissolution of TNT in water at temperatures no greater than 300°C.

The calorimetric work was conducted in small bombs placed in a 300°C bath. Dry TNT detonated after several minutes, while those samples with liquid water present underwent smooth decomposition with no energetic event. This result was in accord with expectation based on the solubility results, and affirmed the inherent safety of the process at least at our small scale.

Calculations of the critical radii for explosion were made for TNT, HMS and PETN at 200 - 350°C based on relations for kinetics of self heating. TNT has a critical radius (r_c) of 0.019 cm at 350°C, meaning that spherical particles exceeding this radius will self heat to explosion at 350°C.

A continuous flow reactor was designed, assembled and tested in studies of the hydrothermolysis of ammonium picrate at 360°C. The data we developed compared well with earlier data we had obtained in another study at lower temperatures in experiments conducted in small batch reactors. All of the data were well fit with an Arrhenius line with the parameters $A = 1.8 \times 10^9\ s^{-1}$ and $E_a = 33$ kcal/mol, which was the rate law followed by both the hydrothermolysis of aqueous picric acid and the initiation to deflagration in neat picric acid. That relationship suggests that the picrate anion is the key species involved in the deflagration.

CONTENTS

LIST OF TABLES

LIST OF FIGURES

INTRODUCTION

SRI International submits this Final Report describing research on the hydrothermolytic destruction of energetic material (EM) conducted on Air Force Contract No. F08637-94-C6050. The disposal of large quantities of waste energetic materials remains a major problem in both the government and private sectors. Open burning, open detonation, and controlled incineration are at present the mainstays of disposal, and their utilization continues to escalate. That growth proceeds, however, in the face of increasing political and public concerns over safety and environmental soundness of the operations.

The study described here was conducted to test a concept for EM disposal that had evolved in earlier SRI studies for the Air Force (Ross et al, 1993, 1996). Framed within the goals of an ultimately safe and environmentally friendly disposal technology, the concept avoids combustion and employs water as the disposal medium. It emphasizes the special properties of liquid water at temperatures from about 300°C up to its critical temperature (T_c) of 374°C. Those properties include the conversion of water to a medium with solvent properties like those of common organic solvents, and increasing hydrolytic reactivity with organic compounds like EMs. The basis of this program is the expectation that this combination of properties will eliminate the explosion hazard by dissolution of the EM in water while simultaneously converting the EM to non explosive products that may be safely discharged following some additional treatment.

The program was conducted in two tasks. In Task 1, we determined the solubility of TNT in hydrothermal media, and then studied the thermal and pressure features of the hydrothermolytic decomposition of TNT. Critical radii calculations for TNT and differential scanning calorimetry studies on TNT were also carried out in this task. In Task 2 we designed and built a bench-scale continuous reactor to operate under hydrothermal conditions determined in Task 1 to test the safe destruction of ammonium picrate.

TASK 1 - DISSOLUTION AND HYDROTHERMAL CALORIMETRY STUDIES

A. THE SOLUBILITY OF TNT IN HYDROTHERMAL MEDIA

Background and Approach

The core of our approach to safe destruction of TNT and other EMs is the recognition that the hazard of thermal destruction lies in the self heating to explosion of the bulk explosive. It follows that elimination of the bulk phase through dissolution in a benign medium where thermal decomposition is moderated by solvent should eliminate the explosion hazard.

The safety of hydrothermolytic disposal of materials like TNT that melt at relatively low temperatures is therefore dependent on the interrelationships of the dynamics of three processes: the internal heating of the bulk explosive, the dissolution of the explosive into the water medium, and the dissolution of water into the bulk TNT. We must therefore consider the phase relationships that exist in water- liquid organic mixtures over the temperature range of interest.

We are unaware of detailed phase studies for TNT/water or for nitroarene/water generally, and so begin our considerations with the phase behavior of benzene/water mixtures, as shown in Figure 1 (Rebert, et al., 1959). Our common experience with the water-benzene system is reflected in the figure at lower temperatures where it exists in three phases, a benzene-rich vapor phase (V) and two liquid phases (L_1 and L_2), respectively benzene- and water-rich. L_1 and the branch above the points of its joining V represent the bulk organic liquid phase, which for TNT would be the component of the system obviously associated with the issues of hazard and safety.

As the temperature is increased the figure shows that the benzene-rich liquid and the vapor phases both increase in water content and compositionally approach each other, becoming a single benzene-rich phase at about 265°C. This phase is a dense, liquid-like phase, and continues with increasing temperature to grow in water content. The water-rich phase at the same time becomes more abundant in benzene. These two phases approach each other as shown, and at the critical point of 306°C/157 atm they become a

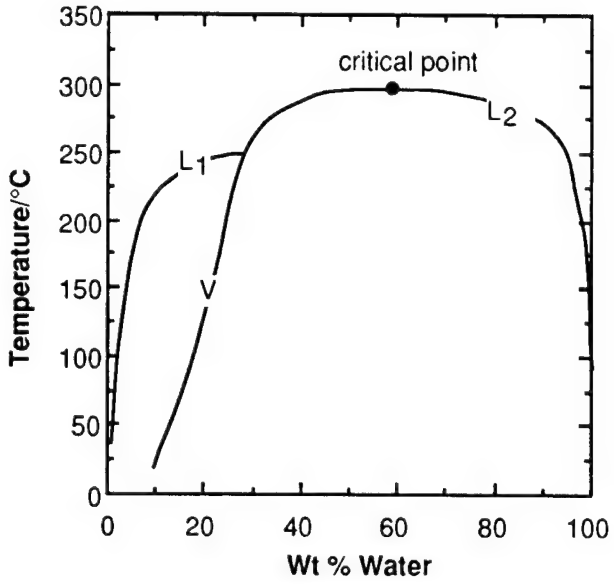

Figure 1. Phase relationships in the water/benzene system. The shaded area represents the bulk organic phase, which in the case of TNT is the hazardous component of the system.

single phase; the organic component and water, in other words, become miscible at all proportions.

Note that the water content of the bulk phase along the L_1 branch up to T_c becomes sizable at relatively low temperatures. Thus at 200°C the water content is several percent, and at 250°C it is up to almost 30%. We can expect TNT to behave in a similar fashion, and because of its nitro-substituents, TNT is likely to be more water-accommodating than is benzene. If this is true increasing dilution of the bulk TNT with water will significantly decrease its tendency to self heat, and that feature alone might be sufficient to provide a safe thermal treatment under relatively modest conditions below T_c. For the realistic case of a 10% slurry of TNT in water, and assuming that the L_2 branch in Figure 1 applies to water/TNT, than all of the TNT becomes soluble below T_c at around 270°C.

Under the worst-case conditions, however, the ultimate safety will depend on complete dissolution of any quantity of TNT at higher temperatures. At this point we shift attention to the dielectric constant of a hydrothermal medium, which is shown in Figure 2. The shaded area shows that the region of dielectric constant values in the 15-30 range, common for polar organic solvents such as alcohols, ketones, and nitroalkanes in which both benzene and TNT are highly soluble. Benzene becomes completely soluble at 250°-300°C, as seen in Figure 6 and TNT should become completely soluble in water in this same region. The study of TNT solubility in

water, was conducted as described below to confirm the conclusions based on dielectric and phase relations.

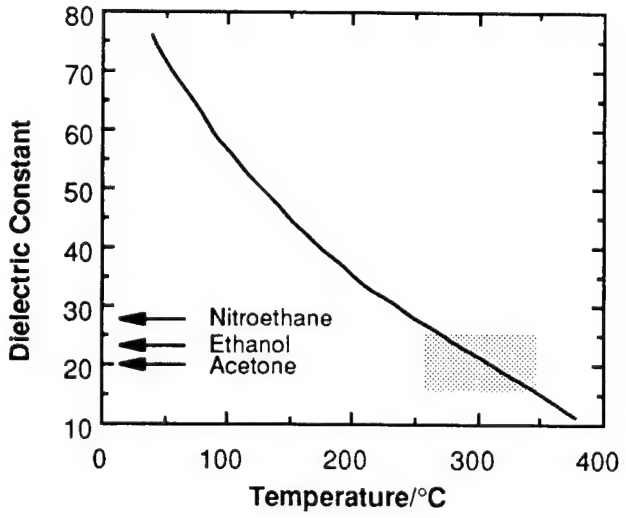

Figure 2. Dielectric constant of water along the liquid/vapor boundary. The organic solvents are at positions representing their dielectric constants at 25°C.

Experimental - Solubility of TNT

Three quartz tubes , 4 mL size (OD = 1 cm) containing 2 wt% TNT in water were prepared by weighing 60 mg TNT into each tube containing 3 mL of water. These tubes were then flame sealed under argon.

The solubility study was conducted in a thermostated aluminum block heater located on the cell compartment of a Hewlett Packard UV spectrophotometer equipped with a diode-array detector. A schematic of the block heater is shown in Figure 3. Each tube containing the TNT slurry was placed in the tube holder thermostated to the required temperature. Undissolved TNT particles settle at the bottom of the quartz tube just below the optical path of the spectrophotometer.

The quartz tubes were removed briefly from time to time and shaken manually to ensure thorough mixing, and the insoluble TNT was allowed to settle before each absorbance measurement. On heating, the solubility of TNT increases and the uv absorbance of the solution increases. Absorbance of dissolved TNT was measured at 150°, 180° and 200°C in separate experiments conducted over periods of several minutes. An earlier kinetic study of TNT

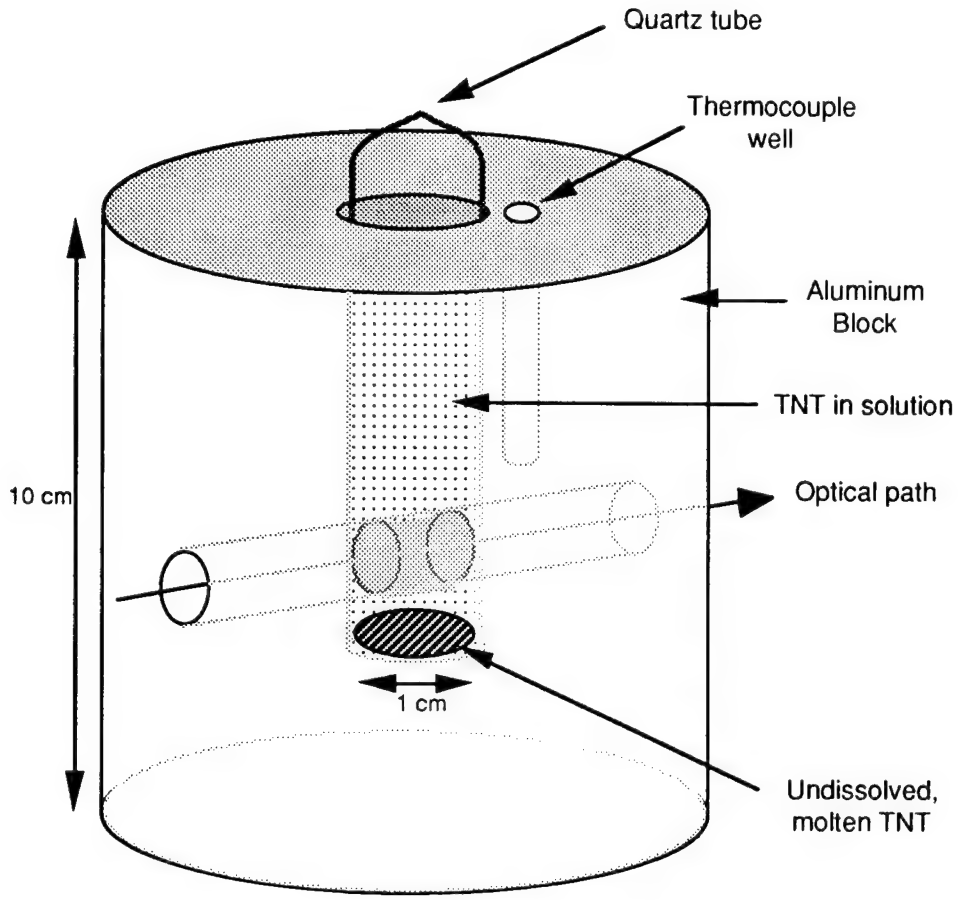

Figure 3. Schematic of the block heater assembly.

hydrothermolysis (Ross, et al., 1993) shown in Figure 4, indicates that the rate of TNT decomposition below about 200°C is sufficiently low to permit reliable measurement of solubility. At higher temperatures, hydrothermolysis rates are too rapid to allow accurate solubility measurements. Absorbances of known concentrations of aqueous TNT solutions were also measured at these temperatures to determine the molar absorption (extinction) coefficients at several wavelengths. Saturated solubilities of TNT were calculated from the absorbances and known extinction coefficients.

Results

Molar extinction coefficients were calculated from the measured absorbance of 0.1% solutions at 150°-200°C and the values are presented in Table 1. Table 1 also presents the TNT solubilities measured at the three temperatures, and, as expected, the values are much higher than those reported at lower temperatures (Fedoroff and Sheffield, 1966; Hill, 1928).

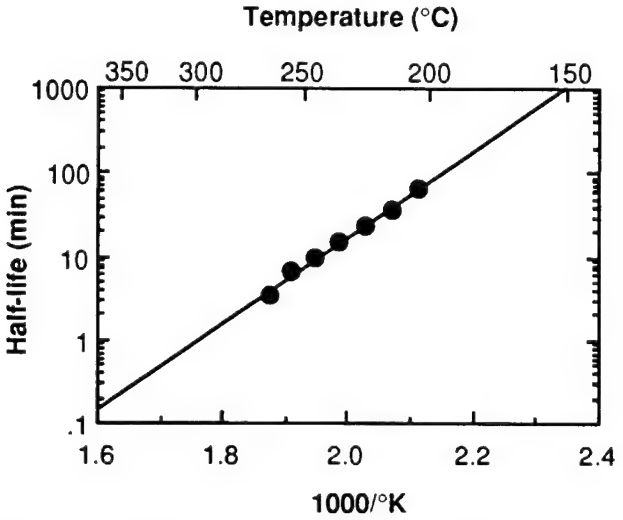

Figure 4. Arrhenius plot for the hydrothermolysis of TNT in homogeneous solution.

TABLE 1

MOLAR ABSORPTION COEFFICIENTS FOR TNT IN WATER[a]

Temperature (°C)	Wavelength (nm)	Absorption coefficient (M^{-1} cm^{-1})	Solubility (wt %)
150	400	111	0.38
180	500	81	0.50
200	510	34	1.50

a. Corrected for expansion of a 0.01% solution of TNT.

Our data, those from the literature, and the L_2 branch for the benzene-water system in Figure 1 (converted from wt % to mole %) are presented in a van't Hoff plot in Figure 5. Solubility data are commonly plotted in this way and fall on straight lines allowing linear extrapolation to temperatures beyond those studied. The linear relationship applies, however, to relatively small temperature ranges where the dielectric of the medium is essentially constant. That effect is suggested in Figure 5 with gray lines, and it is seen that a linear relationship is apparent to 150°C. Above that point the solubility increase for benzene becomes nonlinear. Complete solubility occurs at the critical temperature as the dielectric constant of water decreases into the organic solvent range.

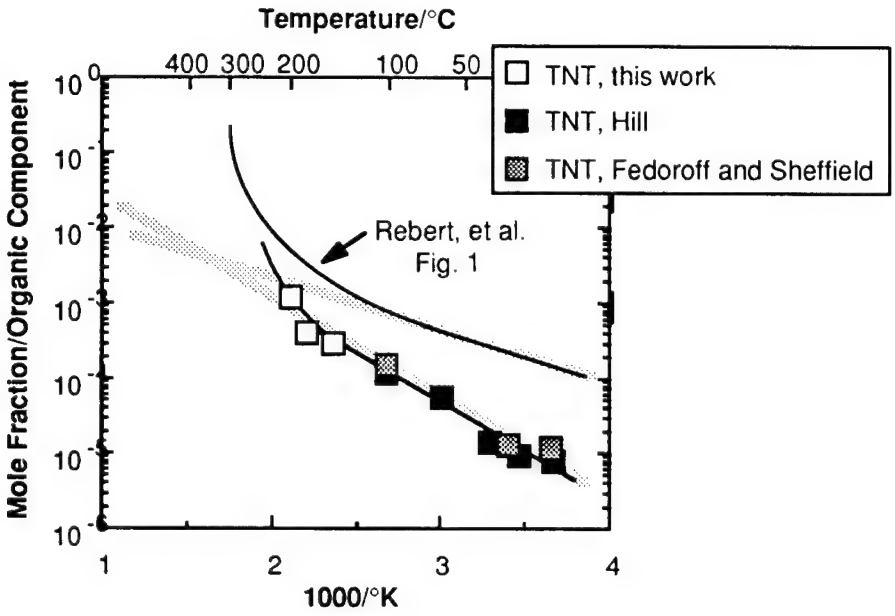

Figure 5 . Solubilities of benzene and TNT in water.

The same argument apply to TNT. As Figure 5 shows, TNT is considerably less soluble in water than is benzene at ambient temperatures, and our data at elevated temperatures appear to fit well with those for lower temperatures. A key feature, however, is the fact that TNT's solubility increases more steeply with temperature; i.e. its enthalpy of solution is greater. This means that TNT will become completely soluble and safely decomposed in water at temperatures in the range of 250°-300°C.

It is useful to conclude this section of this report with data on the products from the exhaustive hydrothermolysis of TNT (Ross, et al., 1996). Table 2 summarizes the data and include products from both hydrothermolysis of TNT alone, and from a mixture of TNT with sodium nitrite, which both eliminated the solid product, and accelerated the hydrothermolysis.

TABLE 2

PRODUCTS FROM THE HYDROTHERMOLYSIS OF TNT AT 300°C/120 MIN[a]

Phase	Product	Fraction of Starting C/N (%)[b]		
		TNT alone	TNT and 3% $NaNO_2$	3% $NaNO_2$ Alone
Carbon				
Gas	CO_2	17	13	-
	CO	1	_c	-
	CH_4	_d	_c	-
Solution	Acetate	4	11	--
	Formate	_c	_c	--
	Glycolate	_c	1	--
	Oxalate	_c	_c	--
	Bicarbonate	_c	61	--
Recovered solid	--	62	None[d]	--
Total C accounted for		84	85	--
Nitrogen				
Gas	N_2O	_c	14	_c
	N_2	30	28	2
Solution	Nitrite	_c	35	90
	Nitrate	_c	2	1
	Ammonium	28	8	_c
Recovered solid	--	31	none[d]	
Total N accounted for		89	87	93

[a] Full conversion.
[b] Reported as final yields in percent of initial carbon and nitrogen.
[c] Trace quantities recovered.
[d] A small quantity of a white solid was recovered and is likely silica derived from the quartz liner of the reactor.

B. THERMAL EFFECTS AND PRESSURE EXCURSIONS DURING THE HYDROTHERMAL DECOMPOSITION OF TNT

Introduction

When dissolution studies suggested that hydrothermal treatment of TNT slurries would be safe, the study then shifted to experimentally demonstrating the validity of the assumptions. It is important to note that a reliable safe disposal system is not necessarily assured on the basis of the thermodynamic estimates of solubility. The promise of safety ultimately rests upon the competitive kinetics of decomposition and dissolution and fluid dynamics, and can be summarized as

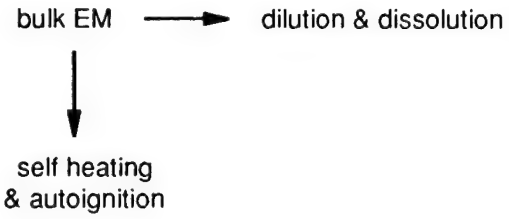

In simple terms, safety comes down to the question of whether or not bulk EM dissolves sufficiently rapidly to complete with the self heating reactions in the EM. (A detailed discussion of self heating and autoignition is provided in Section C of this Task.)

As a test, a series of experiments was undertaken to investigate the thermal consequences of rapidly increasing the temperature and pressure of an aqueous slurry of TNT up to 400°C at 4500 psi. In our initial efforts we utilized a commercial Accelerating Rate Calorimeter (Townsend and Tou, 1980), but we found the large thermal mass of this instrument rendered it unsuitable for the rapid heating of the slurry sample we required.

Ultimately, experiments were conducted in two different reactor systems. The first, conducted in the assembly we refer to as Reactor A, allowed us to use our target 10 wt% TNT levels and provided some familiarity with the system. The second, Reactor B, was designed for smaller TNT quantities where we anticipated autoignition and detonation would take place.

Experimental

Reactor A. TNT as a 10 wt % slurry in water was chosen as a system for initial study. The work was conducted in a self-pressurizing, sealed reactor shown in Figure 6. In this

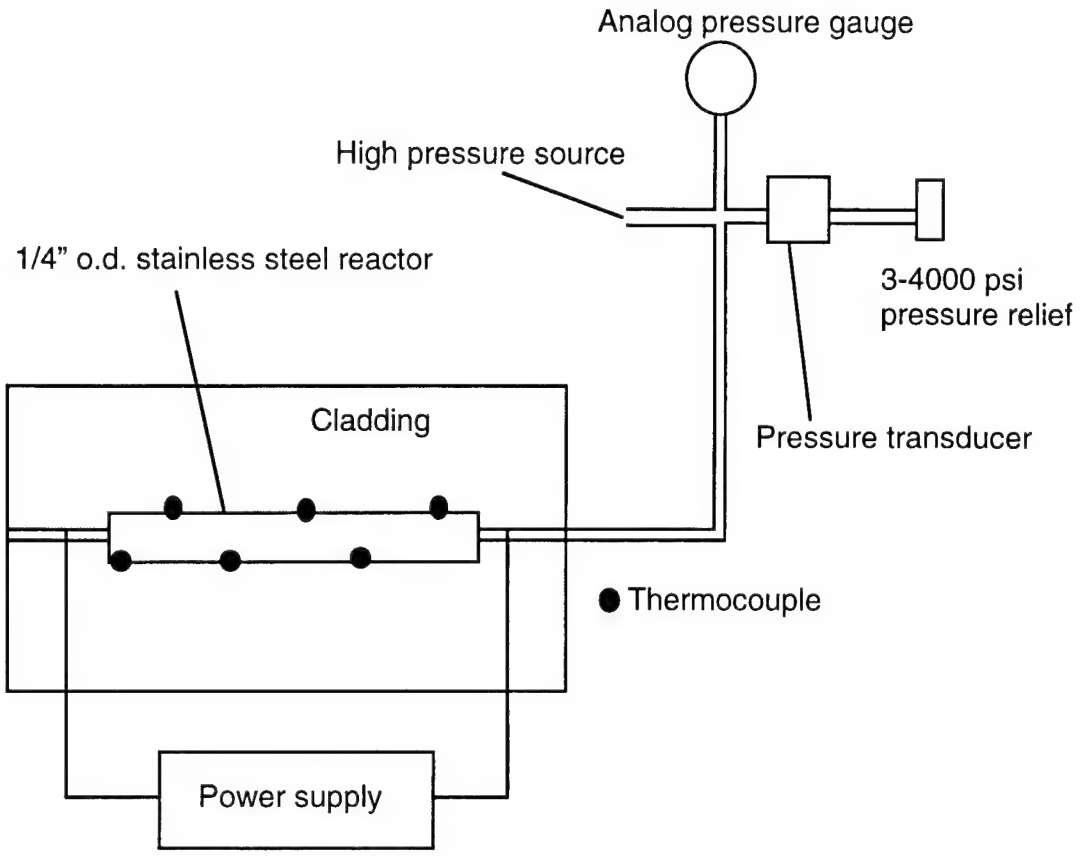

Figure 6. Schematic illustration of closed reaction calorimetry system.

assembly a 1/4" o.d. stainless steel reactor tube approximately 6" long is mounted horizontally and encased in insulating fiber. As shown, the vessel was joined to a manual pressure intensifier, digital and analog pressure gages, and a 5000 psi pressure relief valve with stainless steel capillary tubing. The temperature of the reactor was measured using one or more thermocouples attached directly to the exterior of the reactor. The slurry under test was introduced into the reactor at the outset of the experiment, prior to closing the system. The runs were conducted over a period of 15 min, at which point the temperature and pressure were respectively 450°C and 4500 psia.

Reactor B. This reactor, shown in Figure 7, consisted of an isothermal bath and Controller (Varian Model 3700) for reactor heating, a pressure transducer (Omega Model PX303) and a computer (Macintosh plus) for automatic data collection. Experiments were carried out in 6 mL reactors made from 3/8" stainless steel tubing. Samples were prepared by weighing 80 - 250 mg of TNT in to reactors containing 4 mL of de-ionized water. This volume ratio assured the presence of liquid water throughout the heating periods. Filled reactors were then placed in the thermostated bath at 300° or 350°C and connected to the pressure measuring

equipment. Heat-up times to 300°C for 6 mL stainless steel reactors were 10- 20 min. The pressure was recorded each 0.3 seconds throughout the heating period.

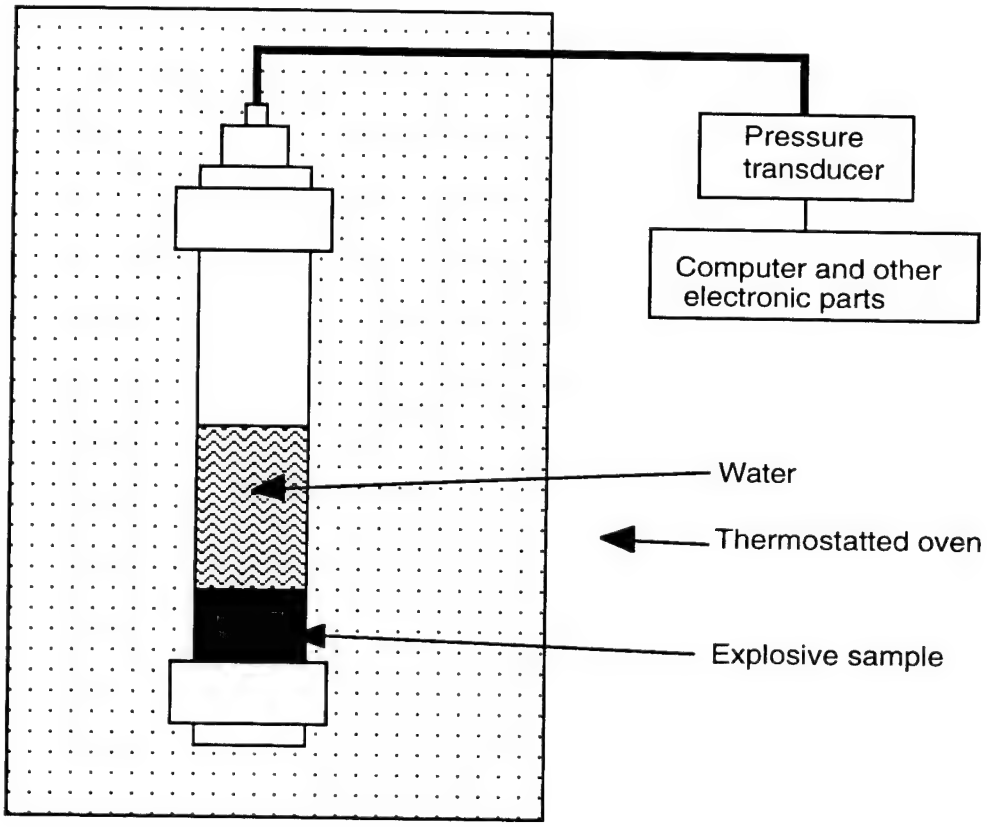

Figure 7. Schematic of reaction B including isothermal bath and the pressure measuring device.

Experiments with dry TNT alone were carried out the same manner, but with no water in the reactor.

Results and Discussion

The first studies were in Reactor A, and the findings in terms of temperature and pressure are presented respectively in Figures 8a and 8b. The figures compare the data with those obtained in control runs with water alone, and included in 8a is a profile for the hydrothermolytic decomposition of TNT employing the Arrhenius expression developed in our earlier Air Force study (Ross, et al., 1993).

$$k = 1.1 \times 10^{7}\, e^{-23.5/RT}\, s^{-1} \qquad (1)$$

The profile was formulated by applying the observed temperature profile in Figure 8a to the Arrhenius expression.

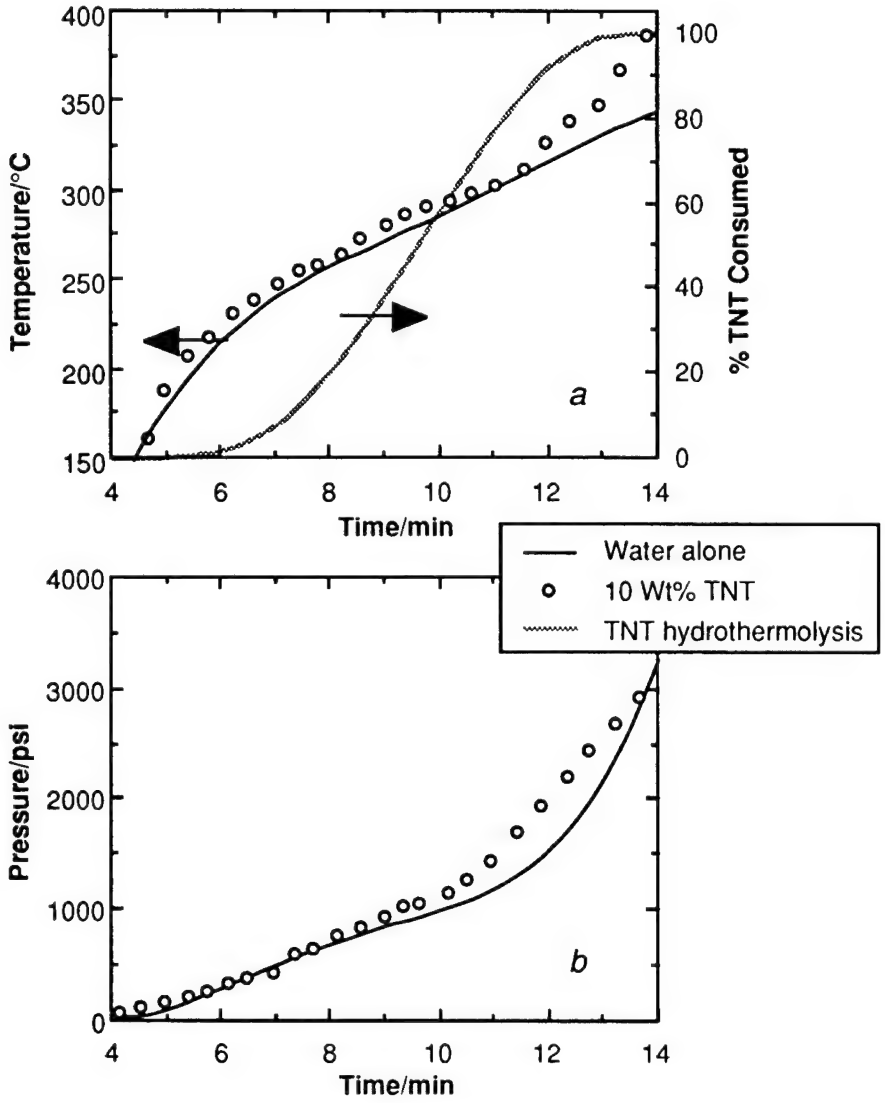

Figure 8. Temperature and pressure changes with heating a 10 wt% TNT slurry in water in Reactor A.

Several features in Figure 8 are worth noting. First, the TNT loss profile shows that most hydrothermolysis takes place between 250° and 300°C. Second, there is no transient pressure or temperature spike, the system at least on this scale appears safe. In 8a it is clear that the temperature of the system with TNT tracks that of the water control up to about 300°. By that time, however, most of the TNT has been hydrothermolytically destroyed. The temperature deviation must therefore come about from the subsequent decomposition of the daughter products. The pressure-time plot in Figure 8b contains a water alone-curve that corresponds to

the temperature profile for the TNT-loaded run represented in Figure 8a. The observed pressure profile shows some deviation from that for water alone, but the shifts are minor.

With these data in hand showing preliminary support for safe hydrothermolysis of TNT in water, studies were initiated in Reactor B. In this case both neat TNT and 2-6 wt% aqueous TNT slurries were used. Results are presented in Table 3 and in Figures 9 and 10.

Table 3 shows that dry heating of TNT leads to sudden energetic events, and the results for the experiment with a 250 mg TNT load are shown in Figure 9. The heat up profile is included in Figure 9, and shows that the reactor came to the target temperature in about 6 min, although it is likely that the chemistry leading to significant thermal decomposition in the bulk TNT began after 4-5 min at temperatures close to 250°C.

At 7.8 min there was an abrupt increase in pressure driving the pressure gage momentarily off scale. This event, most likely a detonation, is consistent with the data of McGuire and Tarver in time-to-explosion studies for TNT (1981). In that work, conducted over the range 200°-350°C with essentially no heatup periods, the time-to-explosion at 250°C was about 10 min, falling to about 1 min at 300°C. The pressure gage quickly recovered, with an immediate offset of about 390 psia representing the product gases. Assuming ideal gas behavior, 3.3 mmols of gases were produced by 1.1 mmols of TNT. Since TNT ($C_7H_5N_3O_6$) is underoxidized this ratio is qualitatively reasonable.

TABLE 3

PRESSURE EXCURSION EXPERIMENTS AT 300° AND 350°C FOR THE DRY AND HYDROTHERMOLYSIS OF TNT

Sample[a]	Temperature (°C)	Final pressure (psi)	Excess pressure (psi)[b]	Mmol product gas[f]	Ratio prod. gas/init. TNT
Dry Decomposition					
214 mg TNT 0.94 mmol	300	.c	250-300[e]	-	-
250 mg TNT 1.10 mmol	300	.c	390	3.3	3.0
Hydrothermal Decomposition					
Water alone	300	1245[d]	-	-	-
Water alone	350	2400[d]	-	-	-
80 mg TNT 0.35 mmol 2.0 wt%	300	1392	147	1.3	3.7
217 mg TNT 0.96 mmol 5.4 wt%	300	1434	189	1.6	1.7
250 mg TNT 1.10 mmol 6.3 wt%	300	1497	252	2.2	2.0
80 mg TNT 0.35 mmol 2.0 wt %	350	2432	34	0.3	0.9

[a]The hydrothermal decompositions were all run in 4.0 mL water. The entries include the mass of TNT, the quantity in mmols, and for the hydrothermal runs the wt% of the slurry.
[b]For the dry runs: Excess pressure = final total pressure - pressure just prior to pressure impulse. For the hydrothermal runs: Excess pressure = final total pressure - pressure of water alone.
[c]Pressure gage momentarily off scale. See Figure 9.
[d]Saturated vapor pressure of water at the final temperature.
[e]The final pressure continued to fall over several minutes.
[f]Presuming ideal gas behavior.

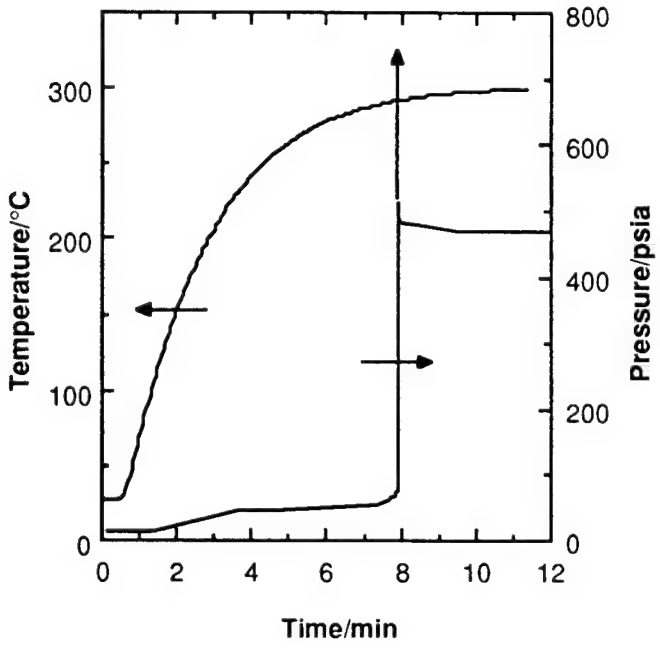

Figure 9. Dry decomposition and generation of pressure with 250 mg of TNT at 300°C.

Figure 10 shows the results of the corresponding hydrothermal decomposition of 2.0 and 6.3 wt% slurries of TNT at 300°C along with the control run with water. Experimental problems prevented our monitoring the temperatures during the runs, but heating power settings were identical for all runs. Figure 10 shows that the profile for the experiment with the 2 wt% loading follows the profile for the control closely, and excess pressure is clearly defined at the end. The reactor temperature reached 300°C in 7-8 min in both cases, and heating rates were therefore similar. The profile for the experiment with the 6.3 wt% loading, on the other hand, shows both a considerable delay in the pressure rise and a slower pressure increase, attaining the target temperature after about 25 min. This longer delay must be due to the larger amount of TNT quantity and the fact that it melts at 82°C, in an endothermic process. The initial decomposition step must also be endothermic, and must contribute to the reduced heatup rate.

It is clear that these two hydrothermal experiments did not result in the energetic events observed in the dry runs. The data from Reactor A, suggests that there is an inherent element of safety in the process. Indeed, the slowly heating, 6.3 wt% run can be viewed as a "worst case" scenario and a significant test of the safety of the hydrothermal process with TNT. TNT clearly must have been present as an insoluble, consolidated mass in these unagitated experiments over much

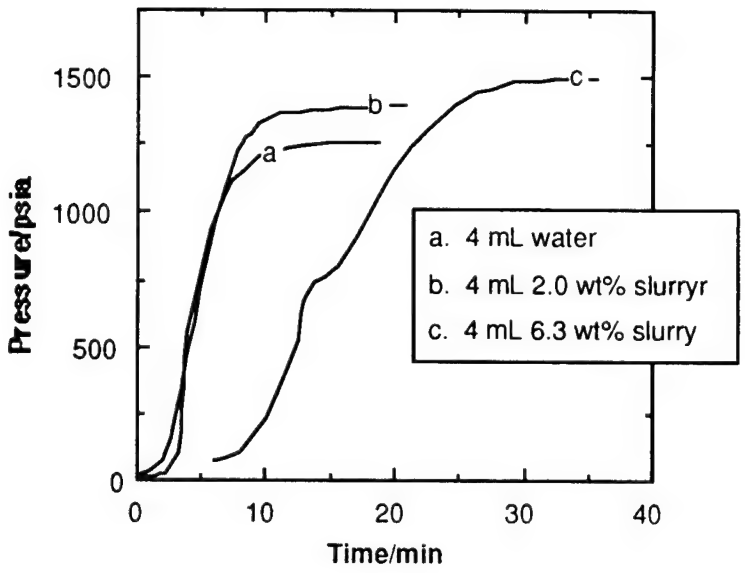

Figure 10. Hydrothermal destruction of TNT at 300°C. Curve a is the control run with water alone; curve b is for a 2 wt% slurry and curve c is for 6.3 wt% slurry.

of the heating period. The bulge evident in the profile for the 6.3 wt% run (Figure (10) suggests that there was some exothermicity, but it is clear that the decomposition took place smoothly and in a manageable manner.

C. CRITICAL RADII CALCULATIONS AND HEAT RELEASE IN TNT SAMPLES USING DIFFERENTIAL SCANNING CALORIMETRY

Self heating of bulk TNT liquid droplets in hot water will occur if heat production exceeds heat loss from the particle. The critical parameters for self heating are calculable from kinetic and heat production parameters. Dissolution of TNT droplets requires time during which self heating may occur if heat production exceeds heat loss caused by the overall exothermic thermal decomposition. Critical parameters for self-heating of TNT have been calculated for TNT to determine the critical radius and temperature parameters needed to minimize self-heating of the TNT droplets. Dissolution of liquid TNT into the aqueous phase will compete with self heating and an accurate estimate of how the two processes compete requires some information concerning rates of dissolution as a function of temperature and droplet size.

Differential scanning calorimetry (DSC) was also used to experimentally determine the thermal behavior of TNT in terms of heat release as a function of temperature, and the heat release-time relationship of different sized samples.

Critical Radii Calculations and the Self Heating of Energetic Materials

The exothermic thermal decomposition of explosives proceeds isothermally as long as the heat of decomposition is lost more rapidly to the surroundings than it is produced. Self heating and explosive decomposition occurs when heat production exceeds heat loss; the temperature of the explosive rises and its rate of decomposition (and heat production) rises exponentially leading to runaway decomposition, deflagration and explosion. For every explosive there is a minimum radius and temperature, r and T_m, above which the exponential increase in decomposition rate with temperature will outpace heat loss, leading to self heating and explosion. The relation between r and T_m and the kinetic reaction parameters for a given explosive is given by the relation (Rogers, 1975)

$$E/T_m = R\ln[r^2 rQZE/T_m^2 ldR] \qquad (2)$$

where E and Z are the activation energy and pre-exponential factor respectively for the decomposition reaction of a specific explosive, r is the radius or thickness of the explosive shape, r is the density, Q the heat released during the self heating reaction, l is the thermal conductivity and d is the shape factor. This equation is a variation of the original heat balance equation, solved by Frank-Kamenetskii (1955) for specific shapes including spheres, slabs and cylinders, for which d has values of 3.32, 0.87 and 2.00 respectively. For the spherical shape, Equation rearranges to Equation (3)

$$r^2 = [(3.32lRT^2/rQZE)e^{E/RT}] \qquad (3)$$

Equation(3) assumes that an infinite heat sink surrounds the explosive; a reasonable assumption for calculating the relation between r and T_m in a hydrothermal slurry.

Solutions for Equation (1 or 2) as plots of T_m versus r (or thickness) give families of lines for different combinations of E and Z. Rogers used Equation (1), with published values of E and Z, to estimate T_m for several explosives. Calculated values of T_m were then compared with measured values of T_m for ten energetic materials with a fixed slab geometry, including HMX, RDX, TNT, and PETN, with good agreement between calculated and measured values. In addition, Rogers lists values for all of the parameters needed in Equation (1), allowing us to calculate, with some confidence, the critical radius of a sphere for these same explosives at several temperatures from Equation (2). The heat production (Q) measured in these slow thermal reactions, ranging from 300 to 600 cal g^{-1} is only a fraction of the heat of explosion for any explosive, presumably because lower temperature reactions are intrinsically less exoergic than

are the high temperature processes responsible for the fast, explosive decomposition and shock wave.

Table 4 lists the values of the critical radius, r, calculated for a spherical explosive from Equation (2), for TNT, HMX and PETN at four temperatures from 200° to 350°C and Figure 11 plots the same data. Values for r for TNT and HMX are similar, but values for PETN are much smaller at all temperatures owing to a much higher value of Z and faster reaction at all temperatures, leading to faster heat generation. Table 4 and Figure 11 show the trade-offs required between slow decomposition even with large radii droplets at low temperature and fast decomposition with high throughput at high temperatures, but where very small radii droplets are required to avoid runaway reactions.

Some confirmation of the validity of the r values would provide an understanding how the energetic materials actually decompose under hydrothermal conditions and what set of operating parameters would ensure both rapid and safe decomposition. In some cases, dissolution in water, followed by decomposition may be a preferred route of decomposition, in which case the rate of solubilization, not the critical radius, would be the important parameter.

Table 4

Critical Radii for Energetic Materials[a]

T (°C)	r, cm (TNT)[b]	r,cm (HMX)[c]	r, cm (PETN)[d]
200	1.22	1.01	0.056
250	0.23	0.075	0.0056
300	0.062	0.009	0.00084
350	0.019	0.0015	0.00018

[a]Equation (2) solved for r with a shape factor d of 3.32 for a sphere.
[b]For TNT, values of I, r, Q, Z and E are 5×10^{-4}, 1.57, 300, 2.5×10^{11} and 34, 400, respectively in units of cm, g, cal, sec and °C.
[c]For HMX values of I, r, Q, Z and E are 7×10^{-4}, 1.81, 500 5×10^{-9} and 52, 700 (see footnote b).
[d]For PETN values of I, r, Q, Z and E are 6×10^{-4}, 1.74, 300, 6.3×10^{19} and 47,000 (see footnote b).

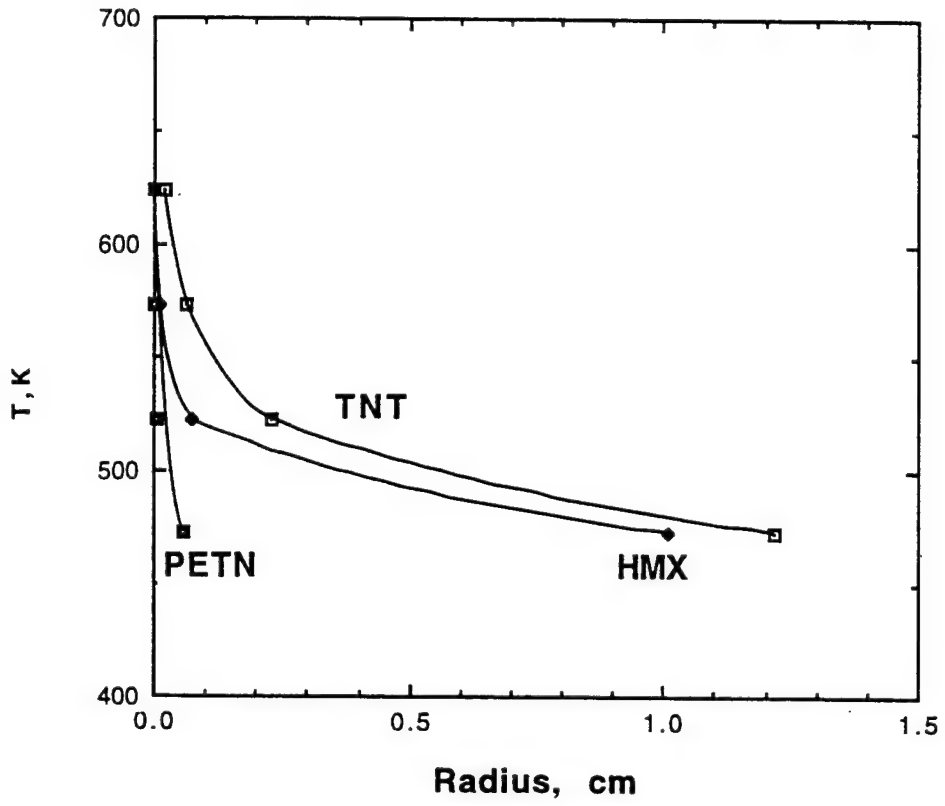

Figure 11. Calculated critical radii for EM at several temperatures.

Differential Scanning Calorimetry

These studies can provide data relating to the heat release-time relationship of different sized samples of an explosive, results bearing directly on the critical radius for self heating and deflagration. These measurements could help indicate whether surrounding the TNT droplet with air or liquid (simulating water) affects the critical radius.

DSC typically requires samples of a mg or less and can measure heat uptake and release as samples melt, freeze, volatilize or decompose with a reproducibility of ± 10%. The TA 910 DSC instrument we used does not have provision for operating under high pressures such as found in water at 200°-300°C. However we can use DSC to measure the effect of EM sample size in air and in an inert, non-volatile fluid on temperature-heat release curves.

Our findings with TNT are summarized in Table 5, while Figure 12 shows a DSC for Run 4 which is typical of those found in all DSC runs.

Table 5

DSC Experiments with TNT[a]

Expt. No.	TNT, mg	T_H, °C[b]	T_{max} °C	H, kJ/mole[c]
1	0.44	294	400	148.4
2	0.85	309	400	303.2
3	0.85	295 (355)	500	308.3 (203)
4	0.47	296 (355)	500	214 (177)

[a] TNT recrystallized with endotherm (m.p.) maximum at 82.25°± 0.1°C.
[b] Temperature of maximum heat release for fast and (slow) releases; see text.
[c] Estimated heat release during fast and (slow) release.

Runs 1 and 2 were heated to 400°C, at 10°C/min. Runs 3 and 4 were heated to 500°C at the same rate. The maximum heat release in all cases is at about 295°C but a secondary, lower and slower heat release shows up at 355°C that was missed in runs 1 and 2. This secondary activity may account for the significant differences we find between values of T_H and H in run pairs 1,2 and 3,4.

Runs 3 and 4 probably gave more accurate measures of temperature and heat release, but these runs have both low and high temperature heat release curves significantly different from each other (308 and 203 versus 214 and 177 kJ/mole). There appears to be a significant size effect on heat release values around 303°C. The large samples (0.85 mg) in runs 2 and 3 agree well with each other, whereas the smaller samples in runs 1 and 4 have significantly smaller heat release values. These differences may be related to the configuration of the liquid TNT in the sample holder

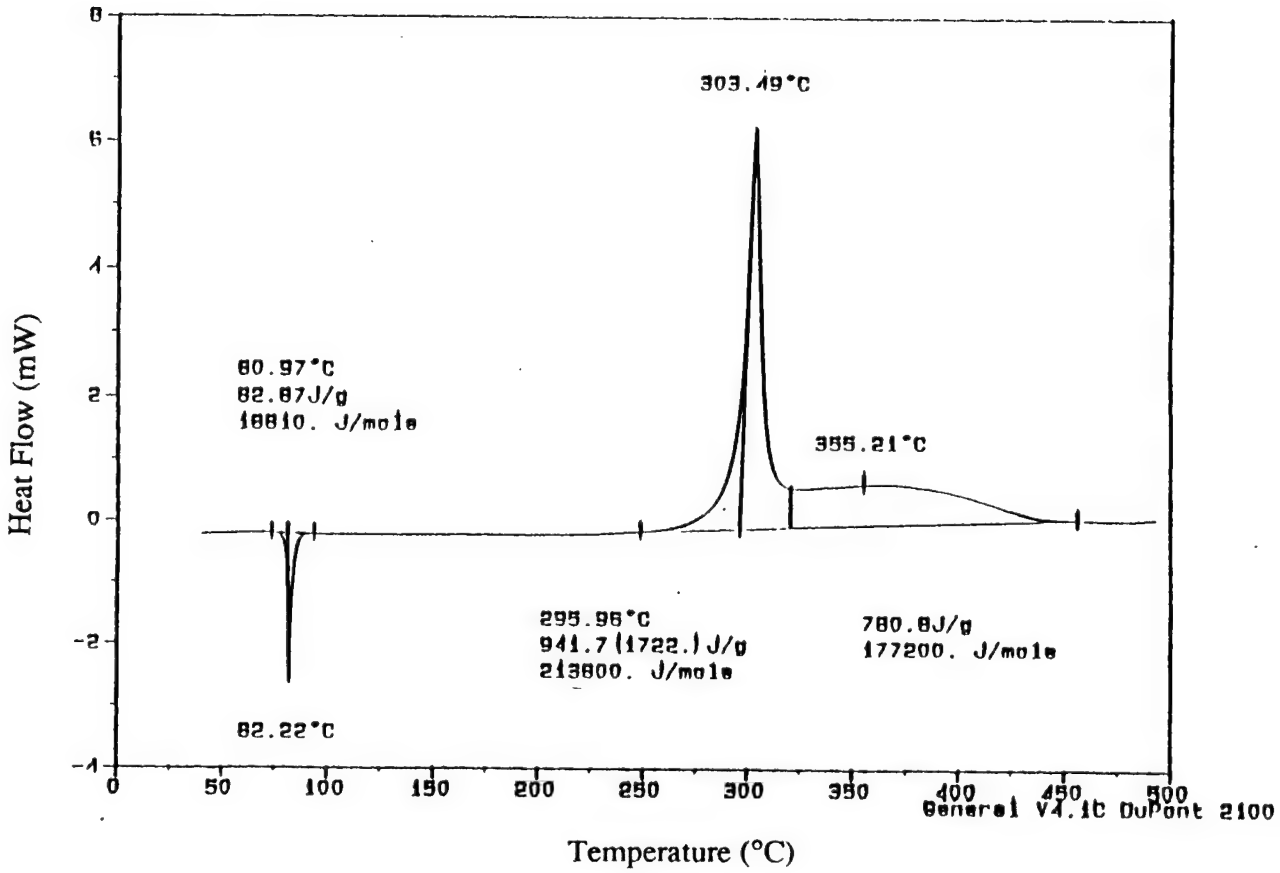

Figure 12. DSC run with 0.47 mg TNT scanned from 25° to 500°C. The endotherm at 82°C corresponds to TNT's melting point.

The combined values for heat release in run 3 is 511 kJ/mole or 540 cal/g, compared with 300 cal/g reported by Rogers (1975) and about 1000 cal/g estimated for heat release on detonation. Table 4 lists a critical droplet radius of 0.062 cm for TNT at 300°C. Our samples have radii of 0.075-0.093 cm if the samples retained a hemispherical droplet configuration, but the more likely configuration for these samples are cylinders with diameters approaching that of the DSC cell of 0.36 cm and with thicknesses of less than 0.01 cm, well below the critical thicknesses of 0.058-0.072 cm estimated from Equation 2 for a cylinder (d = 2).

The exotherm observed at 300°C for samples of this size is in fairly good agreement with the temperature expected for self heating, but the agreement may be fortuitous. Heats of melting for TNT measured in these experiments differ from the reported heat of melting (of 92.5 J/g) (Federoff and Sheffield, 1966) by ± 5-15 J/g, despite careful calibration of the instrument with an indium standard.

A series of DSC runs with 0.5 - 0.7 mg TNT samples gave non-reproducible values of T_H and H, which we believe arises from variable gas evolution and heat loss. In addition, the TNT melt probably assumed different configurations in each trial, increasing the variability of the experiments. Efforts to use aluminum micro pans and covers to confine the TNT melt to a reproducible configuration did not improve the repeatability of DSC runs. We concluded that this approach to validating critical radii calculations would not work unless samples were completely confined in well-defined configuration. No additional DSC measurements were undertaken.

TASK 2 - DESIGN AND OPERATION OF A CONTINUOUS FLOW REACTOR

INTRODUCTION

A continuous flow reactor was designed and assembled to demonstrate the use of the design for studies of the hydrothermolytic destruction of energetic materials, and to obtain accurate kinetic rate data for the destructions. Tubular flow reactors are frequently used to conduct kinetic studies in combustion, pyrolysis , and oxidation chemistry, and the bench scale tubular flow reactors usually operate in the laminar flow regime. Chemical parameters are almost always obtained from tubular flow reactor data by the use of the plug flow idealization in spite of the fluid's parabolic velocity profile within the tubular reactor under laminar flow conditions. Thus, in the use of a laminar flow reactor, it is customary to assume that all the entering molecules spend the same time in the reactor and warm to reactor temperature instantaneously at the inlet, and that the pressure is constant throughout the tube. A large body of research is available on plug flow idealization of tubular-flow reactors, and we designed our reactor using the criteria's given in Culter et al (1988) and Furue and Pacey (1980).

EXPERIMENTAL

Schematic of the Reactor

A schematic of the continuous - flow reactor is shown in Figure 13, and is similar to the supercritical reactor of Ramayya et al. (1987). The reactor tube was made of Hastelloy C-276 , and the tube dimensions are 0.25" OD, 0.109 " ID, 4" long , wall thickness 0.062". The individual parts of the reactor system are given in Appendix A. The reactor tube was arranged horizontally inside of a heated copper tube. Heating was accomplished using a 100 feet of mineral insulated Ni/Cr/Fe wire Aero Coax heating cable wrapped around the copper bar. The copper bar ensures a uniform temperature of the reactor. Four thermocouples were attached to the outside of the reactor, and two thermocouples were attached inside the reactor at the each end to measure the temperature of the effluent. The temperature near the middle of the reactor was controlled by an Omega 808 controller. Typically, a temperature variation of ± 1°C was observed from inlet to the outlet of the reactor providing isothermal conditions. The observed

maximum temperature fluctuation between the two ends of the reactor was <3°C (temperature fluctuation increases with increasing flow rate).

The reagents (waste streams and reactants) are pumped in to the reactor using three different pumps, a Hewlett Packard HP1050 Isocratic pump for high accuracy flows (1± 0.01 mL/min), a Raining high pressure pump (Model HPLX) and an ISCO syringe pump (Model LC-5000). Both HP1050 and Raining pumps are capable of flow rates up to 10 mL/min at pressures up to 8000 psi. ISCO syringe pump was available for pumping pure organics when necessary at very low flows down to 25 μL/min.

The feed streams are separately preheated and mixed in an high pressure cross fitting at the reactor inlet. After the heat treatment, effluent from the reactor passes through a heat exchanger and through a 5 μm filter before reaching a back pressure regulator (Grove Valve and Regulator company, Model 91, 60-6000 psig). The effluent at ambient pressure is then directed to a liquid/gas separator. The separated gas stream is directly connected to a Hewlett Packard 6890 gas chromatograph, and the liquid stream is manually collected for analysis.

Liquid flow rate is measured by weighing the collected liquid fractions and the flow rate is varied from 0.5 -5 mL/min to achieve a range of residence times. Temperature is varied from 300°-450°C, and pressure is in the range 1500-4000 psi. The reactor residence times are often calculated from the linear flow rate and the density of the medium at a given pressure. In the case of water under supercritical conditions, a small change in pressure would lead to a large change in the density, thereby affecting the calculated residence time. Thus, to avoid any error in the residence time measurements, pressures at both ends of the reactor were recorded; the deviation was less than 25 psi.

In residence time calculations we assume that the density of the mixture is that of water for low concentration of organics in water. When the concentration of organics is high, the temperature and pressure in the system allow multiple fluid phases within the reactor. In such cases, a proper equation of state should be applied to determine the temperature and pressure limits within which a single phase exists.

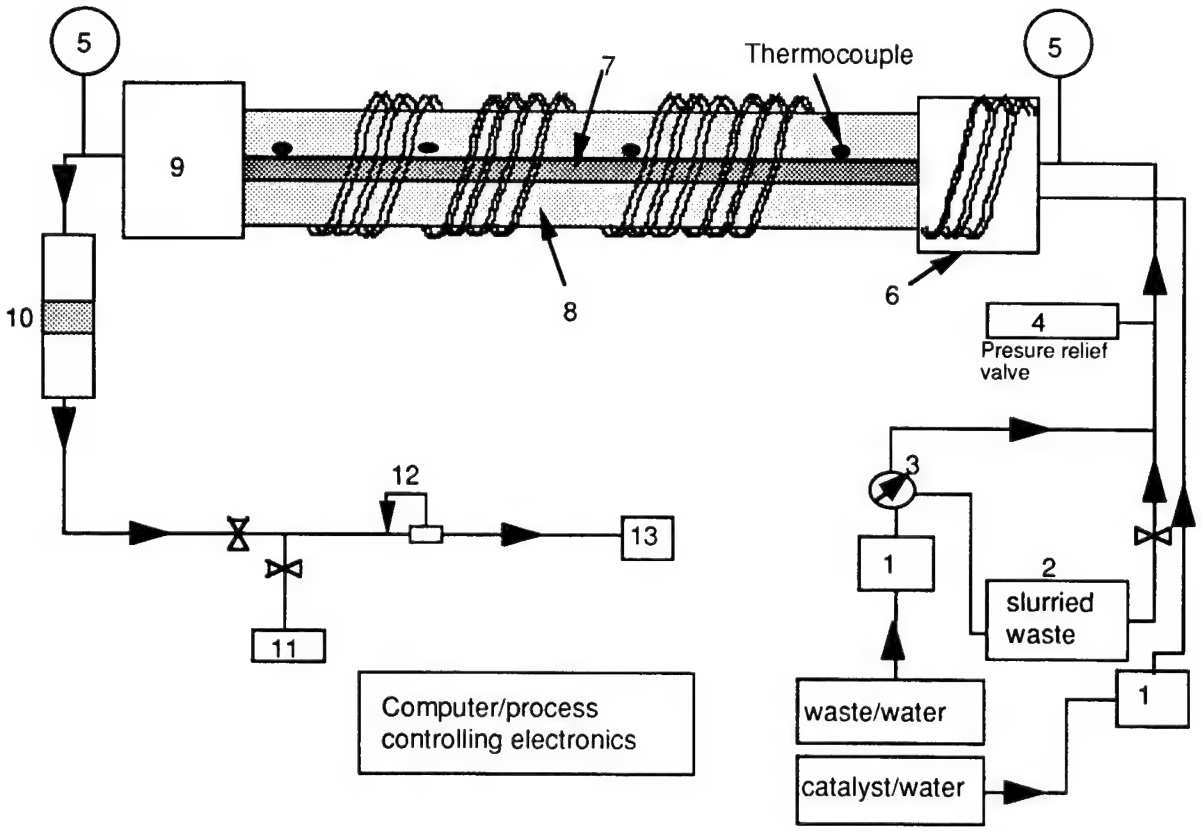

1. HPLC pump
2. Stirred autoclave for slurry introduction,
3. threeway valve for solvent bypass,
4. pressure relief valve,
5. pressure transducer
6. pre-heater,
7. Hastelloy C-276 reactor,
8. heating coil and the copper jacket,
9. heat exchanger,
10. product accumulator,
11. gas cylinders,
12. back pressure regulator,
13. gas liquid separator,

Figure 13. Schematic of the SRI hydrothermal continuous flow reactor.

Ammonium Picrate Studies

A stock solution of ammonium picrate was prepared by mixing equal molar amounts of picric acid and ammonium hydroxide in water. This AMP solution was treated in the flow reactor at 360°C and 3700 psi as described above. Collected treated samples were analyzed for remaining AMP using a Hewlett Packard 1050 liquid chromatograph equipped with a diode-array detector set at 332 nm.

RESULTS

Reactor performance was tested by studying the decomposition of ammonium picrate (AMP or Explosive D) at near supercritical water conditions in the reactor.

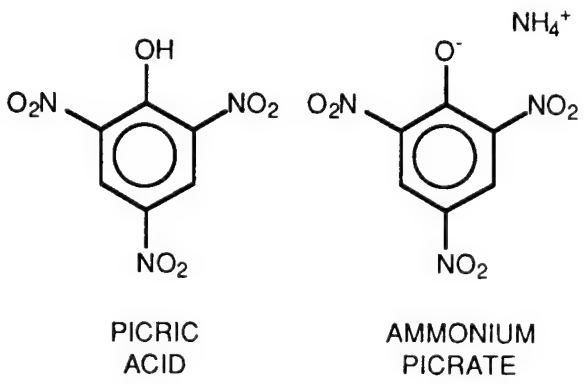

The reactor performed well, as shown in Figure 14 which shows the data obtained at 360°C and 3700 psi initial concentrations of 500 and 750 ppm. The corresponding first order rate constant for the decomposition of AMP at 360°C is 1.4×10^{-2} s^{-1}.

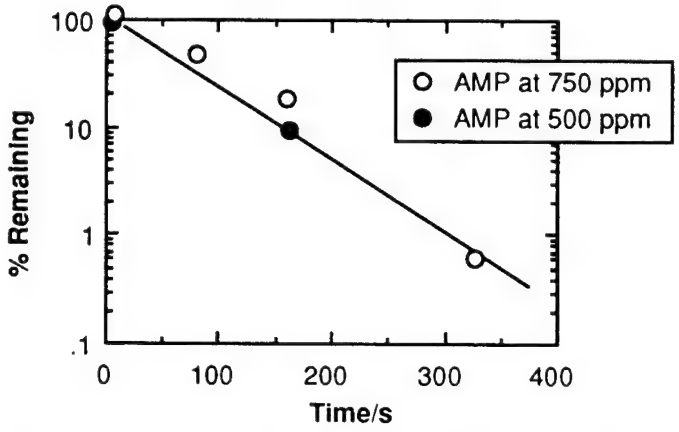

Figure 14. Decomposition of AMP at 360°C and 3700 psi.

This rate constant is shown in an Arrhenius plot in Figure 15 along with lower temperature rate data for aqueous solutions of both AMP and picric acid (PA) obtained in earlier work using batch reactors and a stop-flow UV reactor (Ross, et al., 1996). Figure 15 also includes the rate constants for the initial decomposition of neat, molten PA (mp = 122°C) from Andreev et al. (1963), who observed complex behavior in the decomposition of PA, leading to autoignition. However, hydrothermal decomposition, gave first order behavior up to 99% decomposition.

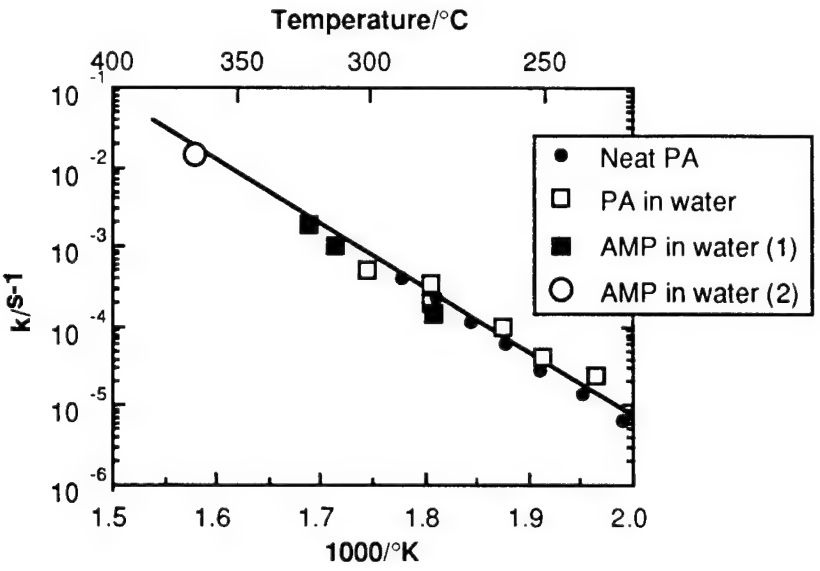

Figure 15. Arrhenius plot for the decomposition of PA and AMP. The source of the neat PA data is Andreev et al., 1963. AMP in water (1) refers to data obtained earlier in Ross, et al., 1996; AMP in water (2) refers to the present work.

The Arrhenius plot shows an excellent linear response over the range of 230°-360°C, providing the Arrhenius parameters $A = 1.8 \times 10^9\ s^{-1}$ and $E_a = 33$ kcal/mol. The linear behavior indicates that the same processes must control decomposition of aqueous PA and AMP throughout this range, and the initial reactions in molten PA. As is discussed below, these findings while preliminary, are instructive in the understanding of the behavior of these and other materials.

The identity of the Arrhenius plots for PA and AMP suggest that they decompose by a common pathway involving the picrate anion. Both compounds form NO_2^- as an intermediate, which appears to promote decomposition of the parent compounds, possibly accounting for the autocatalytic features of some decomposition curves.

CONCLUSIONS

Although it is outside of the scope of this program to provide a quantitative model of the autoignition and decomposition processes, a qualitative understanding of the process can be developed from the findings of this study. We begin with the Arrhenius behavior of AMP and PA just discussed earlier. Since aqueous PA and AMP follow the same Arrhenius law, it follows that the thermolysis of picrate anion is the kinetically significant process in aqueous PA decomposition. From the behavior shown in Figure 15 it is likely that the anion must also be the key to the initiation processes in PA melt. Since that process ultimately leads to autoignition, the anion must somehow be tied to the hazardous behavior, of both PA and AMP.

A simple scheme explaining these findings is

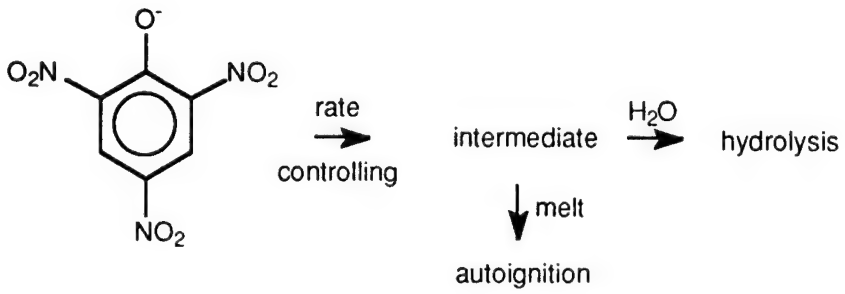

The rate controlling process is thermal conversion of the anion to an intermediate. In the absence of water additional chemistry leads to an exoergic chain process, which then proceeds on to autoignition. With water present the intermediate rapidly and safely hydrolyzes to simple nonenergetic products.

An important thermal pathway in nitroarenes is their isomerization to nitrites (Brill, et al., 1993), and it is conceivable that the intermediate in the scheme has the structure

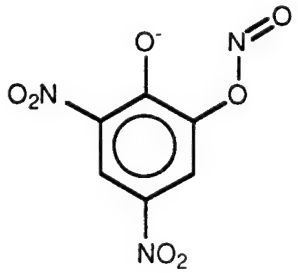

This structure has features that allow it to participate both in continued thermolytic degradation leading to an exothermic chain process in the melt, and hydrolytic degradation in water. We assume that TNT can behave in an analogous manner.

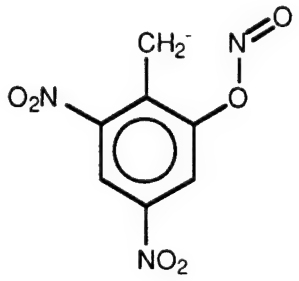

A qualitative sequence of reactions of bulk explosive are summarized in Figure 16. The process proceeds with no external stirring and begins with molten TNT at 82°C. The fate of a spherical droplet of the melt in liquid water at 325°C (1700 psi) proceeds by stages as the droplet warms up to 325°C (the temperature shown in the droplet refers to the temperature at its center). A thermal gradient within the sphere extends to the droplet surface at 325°C. As the droplet is warmed by the water, convection within the melt and at the TNT/water interface, due to thermal gradients, increase mutual solubility and hydrothermolytic decomposition of dissolved TNT, as well as self heating.

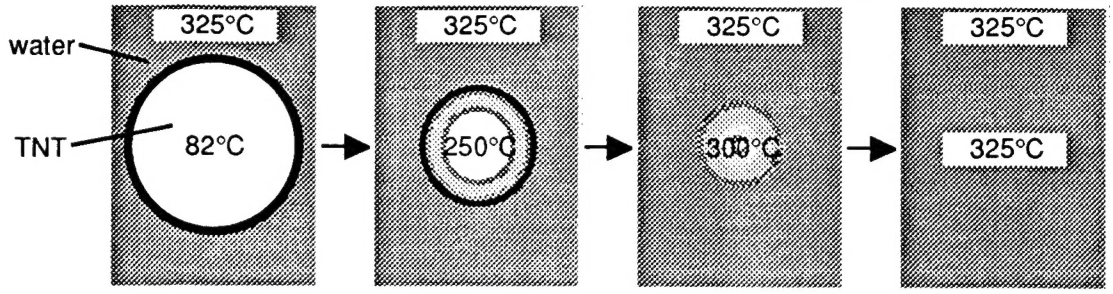

Nature of the system	molten TNT	Significant dilution of TNT phase by water; TNT becomes highly water soluble; thermal gradient promotes convectional forces	Meniscus vanishes; no barrier to convention; mutual dilution accelerated	Convection yields complete solution
Time-to-explosion of bulk TNTa	>5000 hr	22 min	76 s	20 s
Half-life for TNT hydro-thermolysis in aqueous phaseb	>5000 hr	7 min	1 min	24 s

a. McGuire and Tarver, 1981
b. Ross, et al., 1993.

Figure 16. Summary of a proposed sequence in the heating of a TNT/water slurry.

The droplet is heated at its surface, and in the absence of significant self heating in the interior, a temperature gradient to the cooler interior is maintained throughout the process, up to the point of complete solution. Any self heating would provide the opposite condition, with the a portion of the interior warmer than the surface and the aqueous medium. Convectional forces would operate in either case to stimulate mixing, an action that provides a self-governing safety feature.

As the solubility of TNT increases the droplet shrinks and at the same time the bulk TNT is diluted by the increased solubility of water in the melt. On the basis of the considerations discussed earlier 2-3 wt% TNT will become completely soluble at 250-300°C. At this point the meniscus vanishes and thermal convection will give a homogeneous, isotropic solution of TNT in water.

The two chemical processes taking place concurrently are hydrothermolysis of dissolved TNT, and decomposition with self heating in the bulk TNT. Figure 16 includes characteristic times for these processes, and it appears that the rates of the homogenous hydrothermolysis mirror the times-to-explosion quite well. Whether the similar rates reflect some common chemistry is a question to be dealt with in some future study.

The overall phenomenology, however, is clear. The sequential processes in the hydrothermal environment, dilution, dissolution, and hydrothermolytic destruction, could be sufficiently rapid to compete with self heating and deflagration. It appears that on some scale hydrothermal processing of TNT and other EMs is a potentially very safe process that could be the core of a reliable disposal technology.

REFERENCES

Andreev, K. K. and Liu, P., Teoriya Vzryvchatykh Veshchestv, Sb. Satie, 1963. "Thermal Decomposition of Picric and Styphnic Acids," 349-63; Chem Abs. 13761g.

Brill, T. B., James, K. J., 1993. "Thermal Decomposition of Energetic Materials. 662. Reconciliation of the Kinetics and Mechanisms of TNT on the Time Scale from Microseconds to Hours," J. Phys. Chem., **97**, 8759 - 8763.

Cutler, A H., Antal, Jr., M. J., and Jones, Jr., M., 1988. "A Critical Evaluation of the Plug-Flow Idealization of Tubular-Flow Reactor Data," Ind. Eng. Chem., **27**, 691-697.

Fedoroff, B. T.; Sheffield, O. E., 1966. *"Encyclopedia of explosives and related items"*; **editor?** Pictanny Arsenal, New Jersey, p. T261.

Frank-Kamenetskii, D. A. 1955. *"Diffusion and Heat Exchange in Chemical Kinetics,"* Princeton University Press, Princeton, N.J.

Furue, H., and Pacey, P. D., 1980. " Performance of Cylindrical Flow Reactor in a kinetic Study of the Isomerization of Cyclopropane," J. Phy. Chem., **84**, 3139-3143.

Hill, A., 1928. In International Critical Tables, Washburn, E., ed., McGraw-Hill Book Co., New York.

McGuire R. and Tarver, C., 1981. *Proceedings Seventh Symposium (International) on Detonation.* Naval Surface Weapons Center, MP 82-334, 56-64.

Ramayya, S., Brittain, A., Dealmeida, C., Mok, W. and Antal, Jr., M. J.., 1987. "Acid-Catalyzed Dehydration of Alcohols in Supercritical Water," Fuel, **66**, 1364-1371.

Rebert, C. and Kay, W., 1959. "The Phase Behavior and Solubility Relations of the Benzene-Water System," AIChE Journal, **5**, 285-289.

Rogers, R. N., 1975. "Thermochemistry of Explosives," Thermochimica Acta **11**, 131-139.

Ross, D.S., Nguyen, L. K., and Jayaweera, I. S., 1993. "Destruction of Energetic Compounds on Soil and in Water by Reductive Hydrothermal Systems," SRI Final Report 1330, Air Force Contract No. 9-X60-G6898-1.

Ross, D. S., Jayaweera, I. S., Su, M., and Yao, D., 1996. "Advanced Demilitarization Technology - Disposal Syystem for Lab Quantities of Waste Energetic Material," SRI Final Report 5433, AirForce Contract No. F08635-94-C-0017.

Townsend, D. I. and Tou, J. C., 1980. "Thermal Hazard Evaluation by an Accelerating Rate Calorimeter," Thermochimica Acta, **37**, 1-30.

APPENDIX A

DESCRIPTIONS OF THE INDIVIDUAL PARTS OF THE FLOW SYSTEM

Part	Description
(1) HPLC pump	Two HPLC pumps are used here: (i) HP1050 Isocratic pump for high accuracy flows (1± 0.01 ml/min, HP Cat. N0. 440B-43833) , (ii) Waters HPLC pump.
(2)Three-way valve for solvent bypass	Two-way angle valves are used here (Autoclave Enginees Cat. No. 10V20772-GY, pressures upto 11,500 psi.
(3) Feed Chamber	250 mL size magnetically stirred Parr autoclave
(4) Pressure Transducer	Omega Engineering, Cat. No. PX212-6KGV (5000 psi),
(5) Preheater	Omegalux flexible heating tape (max. Temp. 800°C)
(6) Reactor	Hastelloy C-276 reactor 0.25" OD, 0.109 " ID, 4" long , wall thickness 0.062" (Autoclave Engineers Cat. No. MS45-104). 316 SS reactor , 0.25" OD, 0.125" ID, 4' long, wall thickness 0.062" (Autoclave Engineers Cat. No. MS15-055). (Order through Tempresco (9510)-29-3400, Fax: (510)-829-0719, Att: Henry Zappa).
(7) heating coil and copper jacket	ARI AEROCOAX heating cable IHN 125 B-1.6 (Marchi Associates,
(8) Cooling jackect	Chilled water condenser around 1/8" stainless steel tubing
(9) Product accumulator	Line filter , 0.4 μm (Autoclave Engineers Cat. No. SWF4-5, 0.25")
(10) Gas cylinders	Nitrogen and Argon
(11) Back pressure regulator	Grove Valve and Regulator company, Model 91, 60-6000 psig
(12) Gas-liquid separator	Custom built at SRI
(13) gas chromatograph, liquid chromatograph	HP6890 gas chromatograph, HP1050 liquid chromatograph
Miscellaneous parts	
Multiscan board	National Instruments (part # 776910)
Temperature Controllers	Eurotherm model 808,
Panel meter with RS 232	Omega Engineering, Cat # DP41-E-S2
Computer	HP vectra computer with a control board